Electronic Supplementary Material (ESI) for Nanoscale.
This journal is © The Royal Society of Chemistry 2018

Electronic supplementary information (ESI)

Elucidation of interfacial pH behavior at cell/substrate nanogap for in situ monitoring of cellular respiration

*Hiroto Satake, Akiko Saito and Toshiya Sakata**

Department of Materials Engineering, School of Engineering, The University of Tokyo, 7-3-1 Hongo, Bunkyo-ku, Tokyo, Japan 113-8656

*Corresponding author. E-mail: sakata@biofet.t.u-tokyo.ac.jp

CORRESPONDING AUTHOR FOOTNOTE: Affiliation; Department of Materials Engineering, School of Engineering, The University of Tokyo, 7-3-1 Hongo, Bunkyo-ku, Tokyo, Japan, 113-8656, TEL; +81-3-5841-1842, FAX; +81-3-5841-1842

Electronic supplementary information (ESI)

S1. Real-time monitoring of interfacial pH based on cellular respiration

Most biological phenomena *in vivo* are closely related to ionic behaviors such as ion channel activities at the cell membrane or behaviors of various ions in the blood. The direct detection of ions enables the straightforward analysis of various biomolecular recognition events. The principle of a semiconductor-based biosensor based on the field effect, i. e., a field-effect transistor (FET)-based biosensor (bio-FET), can be utilized to directly detect ionic behavior in a solution.[S1,S2] In the last decades, some methods for the electrical measurement of cellular functions using bio-FETs have been reported.[S3-S10] The principle of bio-FETs is based on the potentiometric detection of changes in charge density caused by specific biomolecular reactions at a gate insulator/solution interface. Ionic charges induced at the gate insulator electrostatically interact with electrons in a silicon substrate across a thin gate insulator, resulting in a change in the threshold voltage. In 1970, Bergverd et al. demonstrated a method of the electrical detection of pH variation via the change in the concentration of positively charged hydrogen ions using a FET based on the semiconductor principle.[S1,S2] Such a FET is called an ion-sensitive FET (ISFET), as shown in **Fig. S1(a)**. The semiconductor material is separated with a solution across a gate insulator, the thickness of which is of 100 nm order. The gate insulator is usually composed of an oxide such as SiO_2, Ta_2O_5, or Al_2O_3 or a nitride such as Si_3N_4.[S11] Hydroxyl groups are formed at the surface of the gate insulator in the solution and are very sensitive to hydrogen ions (**Fig. S1(b)**). These positive charges at the gate surface interact electrostatically with electrons in the channel in silicon crystal. The field effect caused by changes in the charge density at the gate induces a change in the threshold voltage (ΔV_T) at a constant drain-source current (I_D). This electrical response of an ISFET to hydrogen ions shows a Nernstian response of about 59.1 mV/pH at room temperature (25 °C) (58 mV/pH in the experimental data in **Fig. S1(c)**). A platform based on a bio-FET device has the advantages of label-free, noninvasive, and real-time measurements, ease of downsizing, and integration with conventional semiconductor microfabrication processes.

As one of the technologies used to monitor cellular respiration in a real-time and noninvasive manner,

an ISFET with a cell-coupled gate (**Fig. S2**) can monitor cellular respiration as a change in pH at a nanoscale cell/gate electrode interface in real time. Since the gate insulator used as an electrode usually consists of an oxide with hydroxyl groups at the surface in a solution, ISFET sensors are sensitive to changes in the concentration of positively charged hydrogen ions on the basis of the equilibrium reaction $-OH_2^+ \leftrightarrow -OH \leftrightarrow -O^-$; consequently, they can be utilized as pH sensors (**Fig. S1(b)**). Thus, the pH variation due to cellular respiration can be monitored at the cell/gate interface through the quantity of released compounds.

Figure S3 shows the change in surface potential (ΔV_{out}) at the gate of the ISFET with the incubation time during cell culture. As a model of cancer cells, human cervical carcinoma (HeLa) and human hepatocellular carcinoma (HepG2) cells were utilized, while bovine chondrocytes and human umbilical vein endothelial cells (HUVECs) were used as a model of normal cells. As shown in **Fig. S3(a)**, ΔV_{out} for every cell-coupled gate ISFET gradually increased after exchanging the culture medium for the purpose of adding nutrients such as glucose to the culture medium, although the control sensor without cells showed almost no electrical response. The positive shift of ΔV_{out} indicated an increase in the concentration of positive charges at the gate surface, that is, an increase in the H^+ concentration at the cell/gate interface. In aerobic respiration, the generated carbon dioxide dissolves in a solution, resulting in the generation of hydrogen ions, and in anaerobic respiration, lactic acid, which exhibits acidity, is released through glycolysis. This is why the pH variation due to cellular respiration was successfully monitored at the cell/gate interface. However, ΔV_{out} depended on the cells used in this study. That is, ΔV_{out} for cancer cells was greater than that for normal cells. In the case of normal cells, it is well known that respiration activity is dominantly conducted through the oxidative phosphorylation pathway in an aerobic environment. On the other hand, cancer cells cause dysbolism, by which cellular respiration occurs through the glycolysis pathway, through which lactic acids are eventually released.[S12-S14] In particular, cancer cells are vigorously activated by suppressing oxidative phosphorylation in mitochondria so as not to induce apoptosis,[S15] resulting in proliferation and metastasis. Therefore, the change in pH based on the metabolic

disorder of cancer cells should be larger than that for normal cells. As mentioned above, ISFET sensors are sensitive to changes in the concentration of positively charged hydrogen ions on the basis of the equilibrium reaction $-OH_2^+ \leftrightarrow -OH \leftrightarrow -O^-$. The gate insulator of the ISFET used in this study was composed of Ta_2O_5/SiO_2 layers, as shown in **Fig. S1(b)**, with thicknesses of 100 and 50 nm, respectively. The oxide surface is mostly covered by hydroxyl groups in a solution, which interact with the hydrogen ions through the equilibrium reaction. As shown in the left graph of **Fig. S1(c)**, the pH was increased in a stepwise manner from 1.68 to 9.18, that is, the measurement solution was exchanged with the next buffer solution at each arrow. The observed correlation between the gate voltage and the pH corresponding to the electrical response is shown in the right graph. The average gate voltage over the last 1 min of each pH response was calculated and is plotted. The gate voltage for pH variation was about 58 mV/pH, near the Nernstian response at 25 °C, which was the ideal response of the interfacial potential at the solution/gate interface. Considering the pH responsivity (58 mV/pH) of the ISFET used in this study, the values of ΔV_{out} shown in **Fig. S3(a)** were converted to the changes in pH for each cell-coupled gate ISFET, as shown in **Fig. S3(b)**. In addition, the nanogap interface is regarded as a closed space between the cell and the gate (the right illustration in **Fig. S2**), where released ions and biomolecules are concentrated, resulting in an increase in the H^+ concentration in the case of cellular respiration. In fact, the pH behavior at the cell/substrate nanogap has been observed by laser scanning confocal microscopy using the phospholipid fluorescein inserted at the cell membrane, as shown in this manuscript. The results show that the pH at the cell/substrate interface gradually decreases (becomes more acidic) and is lower than that at the cell/medium interface. Above all, a prerequisite for the respiratory monitoring of living cells is that the ISFET sensor shows high sensitivity to the pH variation induced at the cell/gate nanogap interface. Therefore, we believe that cellular respiration can be monitored as the change in interfacial pH at the nanogap using the ISFET. This is because in aerobic respiration carbon dioxide dissolves in a solution, resulting in the generation of hydrogen ions, and in anaerobic respiration, lactic acid is released through glycolysis.

Experimental in Section S1

Cell culture

For respiratory monitoring, human cervical carcinoma (HeLa) and human hepatocellular carcinoma (HepG2) cells were used as a model of cancer cells, while bovine chondrocytes and human umbilical vein endothelial cells (HUVECs) were utilized as a model of normal cells.

HeLa and HepG2 cells were cultured in Dulbecco's Modified Eagle's Medium (DMEM, Gibco) with 10% fetal bovine serum (FBS) including 50 U/mL penicillin and 50 μg/mL streptomycin on a conventional cell culture dish (Falcon® Cell Culture Dishes) in an incubator (37 °C, 5% CO_2) for 3 days as the pre-culture, and then transferred to the gate insulator of the ISFET for electrical monitoring, where the same culture medium as that in the pre-culture was added and kept at 37 °C with 5% CO_2 for 24 h. The number of cells seeded on the dish was controlled to 1×10^5 cells/mL for both types of cell.

HUVECs were cultured in endothelial cell growth medium (EGM-2; CC-3162) containing 2% FBS and vascular endothelial growth factor (VEGF, Lonza) on a collagen-coated dish (Falcon® Cell Culture Dishes) in an incubator (37 °C, 5% CO_2), and harvested using trypsin after pre-culture for 1 week. Then, they were transferred to the gate insulator of the ISFET, which was coated with 0.1% gelatin in advance. The number of HUVECs seeded on the dish was controlled to 1×10^5 cells/mL. The preparation of bovine chondrocytes is discussed in the main manuscript and Section S2 in ESI.

Electrical measurement using ISFET device

We used a silicon-based n-channel depletion-mode FET with a Ta_2O_5/SiO_2 (100 nm/50 nm) layer as a gate insulator with a width (W) and length (L) of 340 and 10 μm, respectively. The Ta_2O_5 thin film was used as a passivation layer to prevent leakage current as well as a pH-responsive layer in the buffer solution. The gate voltage (V_G) – drain current (I_D) electrical characteristics were measured using a semiconductor parameter analyzer (B1500A, Agilent). The change in V_G in the V_G-I_D electrical characteristics was estimated as the threshold voltage (V_T) shift, which was evaluated at a constant I_D of 1 mA and a constant of drain voltage (V_D) of 2 V. A Ag/AgCl reference electrode with KCl solution was connected to the measurement solution through a salt bridge (**Fig. S2**). The gate was sufficiently large to detect signals from cells with a diameter of about 10 μm. In particular, W/L at the channel was designed

to ensure sufficient sensitivity of I_D to changes in V_G. Additionally, the gate insulating layers were sufficiently thick to prevent leakage current through the insulating layer caused by the application of bias and the infiltration of ions in the solutions.

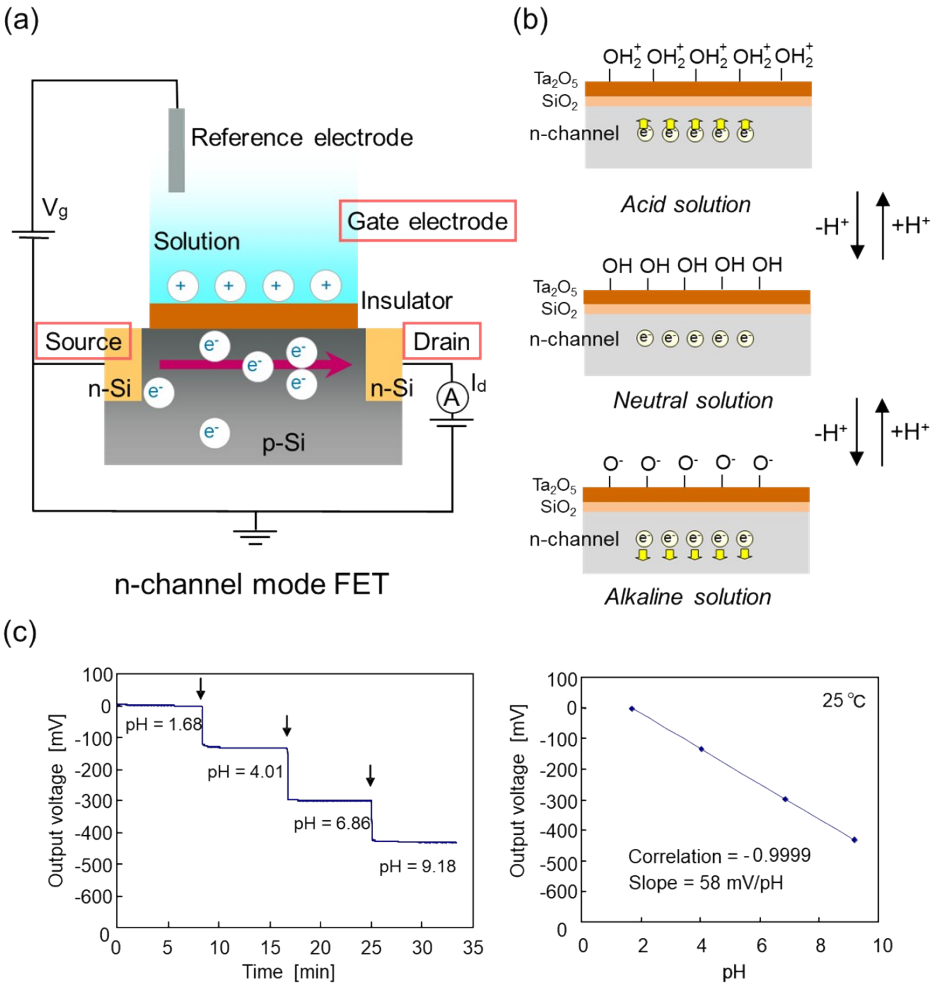

Figure S1 Concept of ion-sensitive field-effect transistor (ISFET) biosensr. (a) Schematic illustration of ISFET biosensor. The gate insulator was composed of Ta_2O_5 and SiO_2 as shown in (b), each thickness of which was 100 and 50 nm, respectively. (b) Solution/gate insulator interface. Oxide surface is mostly covered by hydroxyl groups in solutions, which interact with hydrogen ions as equilibrium reaction. (c) pH response of FET biosensor. pH was exchanged from 1.68 to 9.18 in turn respectively, as shown in the left graph. Measurement solution was exchanged to next buffer solution at the point of arrow. Correlation between gate voltage and pH corresponding to pH response is shown in the right graph. The averaged gate voltages were calculated and plotted for the last 1 minutes in each pH response. The gate voltage for pH variation showed about 58 mV/pH near Nernsian response at 25 °C.

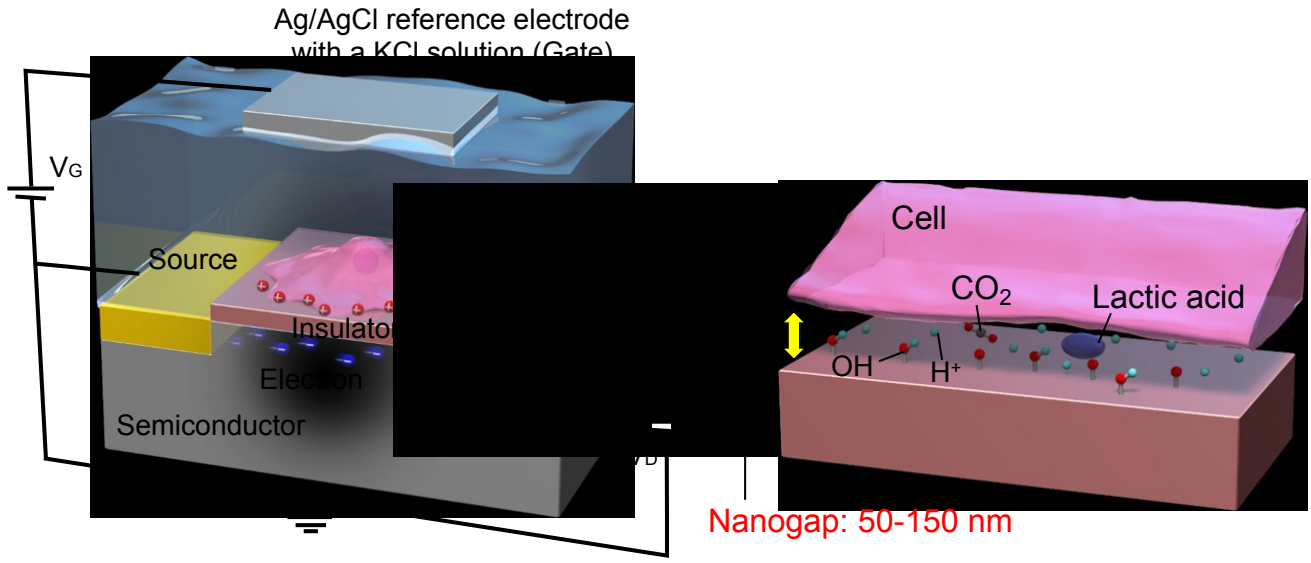

Figure S2 Schematic illustration of cell-coupled gate ISFET.

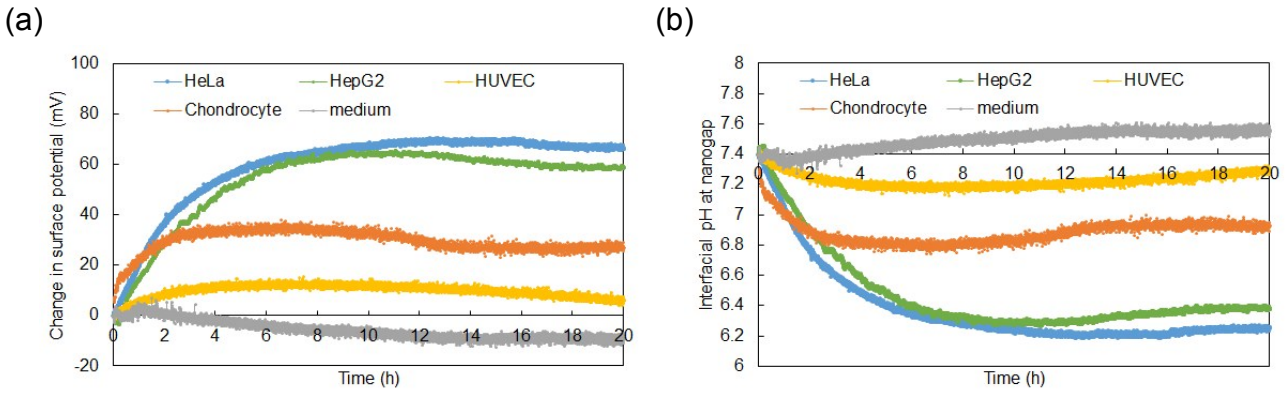

Figure S3 Direct monitoring of interfacial pH with cell-coupled gate ISFET. (a) Change in surface potential at the gate. (b) Real-time monitoring of interfacial pH at cell/gate nanogap. The pH variation was converted from the change in the surface potential shown in (a). In this case, the pH responsivity of the ISFETs used in this study was approximately 58 mV/pH, which was confirmed using the standard buffer solutions with different pH.

S2. Preparation of bovine chondrocytes

Chondrocytes were used as one of the cell model in this study, because they have been studied for the development of articular cartilage in the field of regenerative medicine, which has a limited capacity for self-recovery owing to its avascular and anural nature.[S16,S17] In particular, a regenerative medical technique to transplant cultured autologous chondrocytes have been developed and many studies have been conducted to optimize the condition of culture scaffolds[S18-S20] and the effects of biochemical[S21-S27] and physical stimulations[S28-S31] to improve the quality of cultured cartilage. Our group demonstrated the use of an ISFET with a chondrocyte-coupled gate for monitoring the interfacial pH between the cultured chondrocytes and the gate in real time following the addition of growth factors.[S32]

Isolation of chondrocytes

A bovine hind limb (from a three-month-old calf) was obtained from a local slaughterhouse. The articular cartilage was harvested from the surface (1 mm thickness from the top surface) of the femur and patella bone using a surgical knife. The cartilage was cut into small pieces of about 1 mm^3 and washed three times with Dulbecco's phosphate-buffered saline (DPBS, Gibco) including 50 U/mL penicillin and 50 μg/mL streptomycin and digested with a solution of 0.15% type II collagenase (Worthington) in Dulbecco's modified eagle medium (DMEM, Gibco) including 50 U/mL penicillin and 50 μg/mL streptomycin with gentle shaking for 18 h at 37 °C. The solution was filtrated by a cell strainer (mesh size = 40 μm) and the filtrate was centrifuged with DMEM including 50 U/mL penicillin and 50 μg/mL streptomycin at 1500 rpm for 5 min. After removing the supernatant, chondrocytes were centrifuged twice with DPBS at 1500 rpm for 5 min. Chondrocytes were seeded on a cultivation dish (φ = 10 cm) at a density of 1 x 10^6 cells/dish with DMEM including 10% fetal bovine serum (FBS), 50 U/mL penicillin, and 50 μg/mL streptomycin and cultivated in an incubator (37 °C, 5% CO_2). After the cultivation for two weeks, chondrocytes were collected by trypsin treatment and stored in a freezer (-80 °C) with a cell banker (TaKaRa Bio Inc.) at a density of 1 x 10^6 cells/mL. These cells that underwent one passage were used in experiments.

Pre-culture of chondrocytes

Preserved chondrocytes were seeded on a cultivation dish (φ=10 cm) at a density of 2.5 x 10^5 cells/dish and cultivated in DMEM including 10% FBS, 50 U/mL penicillin, and 50 μg/mL streptomycin in an incubator (37 °C, 5% CO_2). The cells were cultured for one week and the culture medium was replaced with a fresh one every three days. Then, these cells were transferred to the glass-bottomed dish for fluorescence imaging using laser scanning confocal microscopy.

S3. Change in 488 nm/458 nm peak intensity ratio around the boundary between chondrocytes and the glass substrate

Figure S4 shows the change in the 488 nm/458 nm peak intensity ratio around the boundary between chondrocytes and the glass substrate. The ratiometric analysis of fluorescence intensity was carried out using the ratio of the emission intensity at 488 nm to that at 458 nm. The peak of the fluorescence intensity was found at a constant pH by moving an optical slice around the substrate surface (under the cell/substrate interface) to the top of spread cells, where the cell/substrate interface with a nanogap was found, as shown in **Fig. 2(b)**. The change in the interfacial pH (**Fig. 3**) was calculated from the change in the 488 nm/458 nm peak intensity ratio (**Fig. S4**) on the basis of the calibration curve (**Fig. 2(c)**).

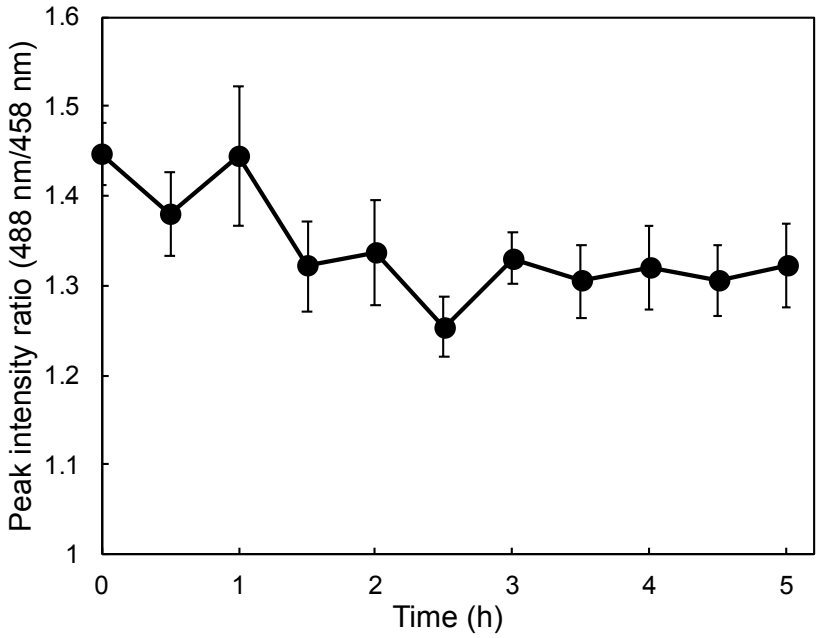

Figure S4 Change in the 488 nm/458 nm peak intensity ratio around the boundary between chondrocytes and the glass substrate

S4. Calibration curve of fluorescence peak intensity for interfacial pH measured by ratiometric analysis (488 nm/458 nm)

For living chondrocytes, the calibration curve of the ratio of fluorescence intensities (488 nm/458 nm) for the interfacial pH on the basis of the peak fluorescence intensity is shown in **Fig. 2(c)**. Similarly, the calibration curves for fixed chondrocytes and HeLa cells are shown in **Figs. S5(a)** and **(b)**, respectively.

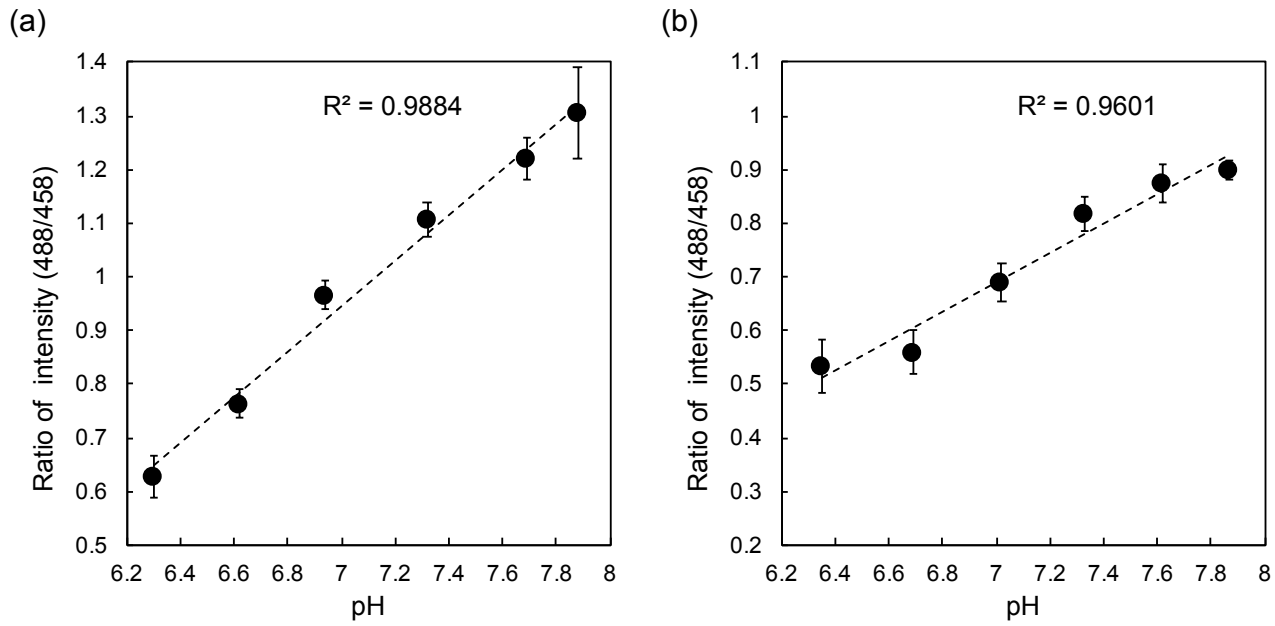

Figure S5 Calibration curve of the ratio of fluorescence intensities (488 nm/458 nm) for the interfacial pH on the basis of the peak fluorescence intensity. (a) Fixed chondrocytes. (b) HeLa cells.

S5. Fluorescence intensity ratio at the plasma membrane of a chondrocyte for the z-axis (z = 0-2.28 μm)

Figure S6 shows the fluorescence intensity ratio at the plasma membrane of a chondrocyte for the z-axis (z = 0-2.28 μm), which indicates the normal direction of the cell/substrate interface, at 1.5 h, following the preculture for 24 h. At slice number 1 (z = 0-0.38 μm), the interface between the cell and the glass substrate was found showing the peak of the fluorescence intensity, as shown in **Fig. 2(b)**. On the other hand, the fluorescence intensity ratios at slice number 3-6 (z = 0.76-2.28 μm) were used to calculate the interfacial pH between the cell and the bulk solution.

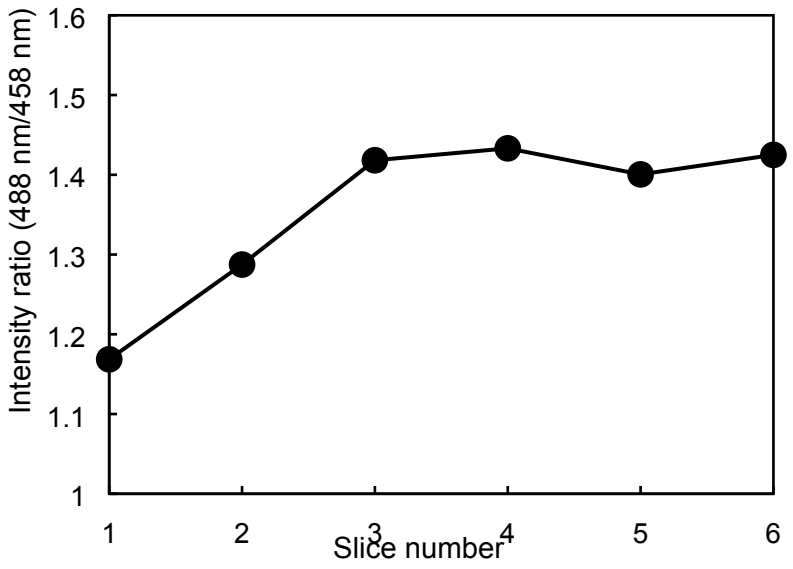

Figure S6 Fluorescence intensity ratio at the plasma membrane of a chondrocyte for the z-axis (z = 0-2.28 μm).

S6. Effect of cell culture medium on pH sensitivity of ISFET

Figure S7 shows ΔV_{out} for pH using the ISFET immersed into a cell culture medium. The ISFET devices were immersed into a cell culture medium for (a) 0 h, (b) 24 h, and (c) 1 w at 25 °C to investigate the effect of nonspecific adsorption of ions and biomolecules such as proteins contained in the medium on the pH sensitivity. DMEM with 10% FBS was utilized as the cell culture medium. As the pH measurement solution, phosphate buffer solutions were prepared by pH values from 5.8 to 8.0 by controlling the mixing ratio of Na_2HPO_4 to KH_2PO_4. The standard buffer solutions with pH values of 4.01, 6.86, 7.41, 9.18 and 10.01 (Wako Pure Chemical Industries, Ltd.) were also prepared. The measurement was carried out in accordance with our previous works.[S1-S10] At 0 h, the ISFET device, which was not immersed in the cell culture medium, showed 59.4 mV/pH near Nernstian response at 25 °C. Moreover, the pH sensitivities were almost maintained around 58 mV/pH, even when the ISFET devices were immersed into the cell culture medium for 24 h and 1 w. Therefore, the effect of nonspecific adsorption of proteins contained in the medium on the pH sensitivity can be almost neglected. In general, the FET biosensors have the limitation of detections depending on the Debye length expressed by

$$\lambda = \sqrt{\frac{\varepsilon_0 \varepsilon_r k_B T}{2 N_A e^2 I}}, \quad (1)$$

where I is the ionic strength of the electrolyte, ε_0 is the permittivity of free space, ε_r is the dielectric constant, k_B is the Boltzmann constant, T is the absolute temperature, N_A is the Avogadro number and e is the elementary charge.[S33]

In this case, the changes in charges based on biomolecular recognition events can be detected within the Debye length, which depends on ionic strengths in a solution; therefore, the electrical charges based on macromolecules such as proteins can be easily shielded by counter ions in a cell culture medium with high ionic strengths. This means that the cell-based ISFET sensors are insensitive to adsorbed proteins on the gate in a cell culture medium because there are also nonspecific adsorptions of proteins on the gate during pre-culture. However, the ISFET sensor, which has the oxide membrane as the gate insulator, is sensitive to pH even when it is used in a cell culture medium, because the size of hydrogen ion is the

smallest among ions and its equilibrium reaction with hydroxyl group at the oxide is expected without the influence of adsorbed proteins. Thus, the cell-based ISFET sensors can specifically monitor the cellular respiration activity as the change in the interfacial pH at the cell/oxidized gate nanogap in real time, preventing nonspecific signals derived from proteins because the Debye length is smaller at a higher ionic strength.

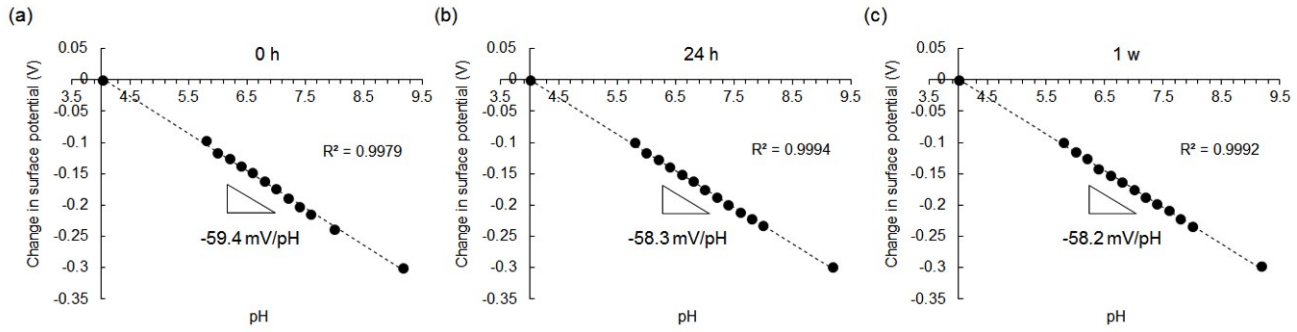

Figure S7 Change in the surface potential for pH using the ion-sensitive field-effect transistor (ISFET) immersed into a cell culture medium.

References

S1 P. Bergveld, *IEEE Trans. Biomed. Eng.*, **BME-17**, 70 (1970).

S2 P. Bergveld, *Sens. Actuators B*, **88**, 1 (2003).

S3 P. Fromherz, A. Offenhäusser, T. Vetter, and J. Weis, *Science*, **252**, 1290 (1991).

S4 B. Straub, E. Meyer, and P. Fromherz, *Nat. Biotechnol.*, **19**, 121 (2001).

S5 T. Sakata, and Y. Miyahara, *Anal. Chem.*, **80**, 1493 (2008).

S6 T. Sakata, I. Makino, S. Kita, and Y. Miyahara, *Microelectron. Eng.* **85**, 1337 (2008).

S7 B. Hofmann, V. Maybeck, S. Eick, S. Meffert, S. Ingebrandt, P. Wood, E. Bamberg, and A. Offenhäusser, *Lab Chip*, **10**, 2588 (2010).

S8 J. M. Rothberg, W. Hinz, T. M. Rearick, J. Schultz, W. Mileski, M. Davey et al., *Nature*, **475**, 348 (2011).

S9 T. Sakata, I. Makino, and S. Kita, *Eur. Biophys. J.*, **40**, 699 (2011).

S10 T. Sakata, A. Saito, J. Mizuno, H. Sugimoto, K. Noguchi, E. Kikuchi, and H. Inui, *Anal. Chem.*, **85**, 6633 (2013).

S11 P. T. McBride, J. Janata, P. A. Comte, S. D. Moss, and C. C. Johnson, *Anal. Chim. Acta*, **108**, 161 (1979).

S12 Hsu, P.P. & Sabatini, D.M.(2008)Cell, 134, 703–707.

S13 Cairns, R.A., Harris, I.S., & Mak, T.W. (2011) Nat. Rev. Cancer, 11, 85–95.

S14 Munoz-Pinedo, C., Mjiyad, N.E., & Ricci, J.-E.(2012)Cell Death Disease, 3, e248.

S15 Vaughn, A. E. & Deshmukh, M. Glucose metabolism inhibits apoptosis in neurons and cancer cells by redox inactivation of cytochrome c. Nature Cell Biol. 10, 1477–1483 (2008).

S16 E. B. Hunziker, Osteoarthr. Cartilage 1999, 7, 15.

S17 M. Brittberg, A. Lindahl, A. Nilsson, C. Ohlsson, O. Isaksson, L. Peterson, New, Engl, J. Med., 1994, 331, 889.

S18 M. D. Buschmann, Y. A. Gluzband, A. J. Grodzinsky, J. H. Kimura, and E. B. Hunziker, J. Orthop. Res. 1992, 10, 745.

S19 J. K. Mouw, N. D. Case, R. E. Guldberg, A. H. K. Plaas, M. E. Levenston, Osteoarthr. Cartilage 2005, 13, 828.

S20 J. Elisseeff, W. Mclntosh, K. Anseth, S. Riley, P. Ragan, R. Langer, J. Biomed Mater Res. 2000, 51, 164.

S21 A. M. Freyria, M. C. Ronziere, S. Roche, C. F. Rousseau, D. Herbage, J. Cell. Biochem. 1999, 76, 84.

S22 J. J. Jeffrey, G. R. Martin, Biochim. Biophys. Acta 1966, 121, 269.

S23 A. G. Glark, A. L. Rohrbaugh, I. Otterness, V. B. Kraus, Matrix Biol. 2002, 21, 175.

S24 J. D. Kisiday, B.Kurz, M. A. DiMicco, and A. J. Grodzinsky, Tissue Eng. 2005, 11, 141.

S25 X. Liu, J. Liu, N. Kang, L. Yan, Q. Wang, X. Fu, Y. Zhang, R. Xiao, Y. Cao, Int. J. Mol. Sci. 2014, 15, 1525.

S26 K. H. Chua, B. S. Aminuddin, N. H. Fuizina, B. H. I. Ruszymah, Eur. Cells Mater. 2005, 9, 58.

S27 P. C. Yaeger, T. L. Masi, J. L. de Oritz, F.Binette, R.Tubo, and J. M. McPherson, Exp. Cell. Res. 1997, 237, 318.

S28 S. D. Waldman, C. G. Spiteri, M. D. Grynpas, R. M.Pillar, R. A. Kandel, J. Orthop. Res. 2003, 21, 590.

S29 B. D. Elder, K. A. Athanasiou, Tissue Eng. 2009, 15, 42.

S30 T. Ikenoue, M. C. Trindade, M. S. Lee, E. Y. Lin, D. J. Schurman, S. B. Goodman, R. L. Smith, J. Orthop. Res. 2003, 21, 110.

S31 S. Mizuno, T. Tateisi, T. Ushida, J. Glowacki, J. Cell. Phys. 2002, 193, 319.

S32 H. Satake, A. Saito, S. Mizuno, T. Kajisa, T. Sakata, *Jpn. J. Appl. Phys*. **2017**, *56*, 04CM03.

S33 P. Debye and E. Hu¨ckel, *Phys. Zeit.* **1923**, *24*, 185.